Weibel-Palade Body Localized Syntaxin-3 Modulates Von Willebrand Factor Secretion From Endothelial Cells

17 authors, including:

Maaike Schillemans
Sanquin Blood Supply Foundation
5 PUBLICATIONS **9** CITATIONS

SEE PROFILE

Ellie Karampini
Sanquin Blood Supply Foundation
4 PUBLICATIONS **7** CITATIONS

SEE PROFILE

Bart Laurens van den Eshof
Sanquin Blood Supply Foundation
10 PUBLICATIONS **30** CITATIONS

SEE PROFILE

Anastasia Gangaev
Netherlands Cancer Institute
3 PUBLICATIONS **3** CITATIONS

SEE PROFILE

Some of the authors of this publication are also working on these related projects:

Project Intradermal vaccination using nanoparticles and hollow microneedles View project

Project PROFILE Consortium View project

Weibel-Palade Body Localized Syntaxin-3 Modulates Von Willebrand Factor Secretion From Endothelial Cells

Maaike Schillemans, Ellie Karampini, Bart L. van den Eshof, Anastasia Gangaev,
Menno Hofman, Dorothee van Breevoort, Henriët Meems, Hans Janssen, Aat A. Mulder,
Carolina R. Jost, Johanna C. Escher, Rüdiger Adam, Tom Carter, Abraham J. Koster,
Maartje van den Biggelaar, Jan Voorberg, Ruben Bierings

Objective—Endothelial cells store VWF (von Willebrand factor) in rod-shaped secretory organelles, called Weibel-Palade bodies (WPBs). WPB exocytosis is coordinated by a complex network of Rab GTPases, Rab effectors, and SNARE (soluble NSF attachment protein receptor) proteins. We have previously identified STXBP1 as the link between the Rab27A-Slp4-a complex on WPBs and the SNARE proteins syntaxin-2 and -3. In this study, we investigate the function of syntaxin-3 in VWF secretion.

Approach and Results—In human umbilical vein endothelial cells and in blood outgrowth endothelial cells (BOECs) from healthy controls, endogenous syntaxin-3 immunolocalized to WPBs. A detailed analysis of BOECs isolated from a patient with variant microvillus inclusion disease, carrying a homozygous mutation in *STX3* (STX3$^{-/-}$), showed a loss of syntaxin-3 protein and absence of WPB-associated syntaxin-3 immunoreactivity. Ultrastructural analysis revealed no detectable differences in morphology or prevalence of immature or mature WPBs in control versus STX3$^{-/-}$ BOECs. VWF multimer analysis showed normal patterns in plasma of the microvillus inclusion disease patient, and media from STX3$^{-/-}$ BOECs, together indicating WPB formation and maturation are unaffected by absence of syntaxin-3. However, a defect in basal as well as Ca^{2+}- and cAMP-mediated VWF secretion was found in the STX3$^{-/-}$ BOECs. We also show that syntaxin-3 interacts with the WPB-associated SNARE protein VAMP8 (vesicle-associated membrane protein-8).

Conclusions—Our data reveal syntaxin-3 as a novel WPB-associated SNARE protein that controls WPB exocytosis.

Visual Overview—An online visual overview is available for this article. (*Arterioscler Thromb Vasc Biol*. 2018;38: 1549-1561. DOI: 10.1161/ATVBAHA.117.310701.)

Key Words: endothelial cells ■ SNARE protein ■ syntaxin ■ von Willebrand factor ■ Weibel-Palade body

V WF (von Willebrand factor) is a multimeric adhesive glycoprotein that is critically involved in hemostasis by mediating adhesion of platelets to sites of vascular damage and by acting as a chaperone for coagulation factor VIII in plasma. The importance of VWF for vascular homeostasis is illustrated by the pathophysiological phenotypes that are associated with abnormal levels of circulating VWF. Low levels of VWF are associated with bleeding, such as in the inherited bleeding disorder von Willebrand disease, while elevated levels of VWF are associated with increased risk of thrombosis and cardiovascular disease.[1] The majority of VWF is synthesized by endothelial cells, where it is stored in secretory organelles called Weibel-Palade bodies (WPBs). VWF, together with several inflammatory and angiogenic mediators, is rapidly released from WPBs on shear stress or damage to the vessel wall.[2]

The mechanisms that regulate biogenesis and exocytosis of WPBs are complex and poorly understood. During biogenesis and maturation, WPBs recruit a set of Rab GTPases (Rab27A, Rab3B/D, and Rab15) and Rab effectors (MyRIP, Slp4-a, and Munc13-4) that mediate interactions with the cytoskeleton and plasma membrane. Recruitment of these molecules coincides with the acquisition of WPB secretion competence and provides the link with SNARE (soluble NSF attachment protein receptor) complex proteins.[3–9] SNARE complexes are molecular machines that catalyze the fusion of lipid bilayers, which plays a central role in the exocytosis of secretory vesicles. They typically consist of 4 SNARE helices: 1 provided by a v-SNARE/R-SNARE on the donor compartment (VAMPs [vesicle-associated membrane proteins]) and 3 Q-SNAREs provided by a t-SNARE complex (1 by syntaxins and 2 by SNAP25

DOI: 10.1161/ATVBAHA.117.310701

Nonstandard Abbreviations and Acronyms	
BOEC	blood outgrowth endothelial cell
HUVEC	human umbilical vein endothelial cell
MVID	microvillus inclusion disease
SNARE	soluble NSF attachment protein receptor
VWF	von Willebrand factor
WPB	Weibel-Palade body

homologues) on the acceptor compartment. Assembly of v- and t-SNAREs into a parallel 4 helix bundle produces a mechanical force that brings the vesicle and target membranes in close proximity, lowering the energetic barrier for fusion. Several SNARE and SNARE-associated proteins have been implicated in WPB exocytosis.[10–14] Despite this, we currently do not know the exact composition of the WPB exocytotic machinery and how all these individual components together orchestrate WPB release. Recently, syntaxin-3 was found as part of a complex with STXBP1 and the Rab27A-effector Slp4-a, which both have been identified as positive regulators of WPB exocytosis.[7,12]

In this study, we show that syntaxin-3 localizes to WPBs. VWF secretion is significantly impaired in ex vivo STX3$^{-/-}$ endothelial cells derived from a patient with variant microvillus inclusion disease (MVID), whereas WPB abundance and morphology are unaffected. We identified VAMP8, another WPB-localized SNARE, as an interaction partner of syntaxin-3. Together, the data identify syntaxin-3 as a new component of the SNARE machinery regulating WPB exocytosis and VWF secretion.

Materials and Methods

All further supporting data are available within the article and its online supplementary files.

The whole-proteome analysis.raw MS files and search/identification files obtained with MaxQuant are available through the ProteomeXchange Consortium (http://proteomecentral.proteomexchange.org/cgi/GetDataset) via the PRIDE partner repository[15] with the data set identifier PXD006176.

Antibodies

Antibodies used in this study are listed in Table I in the online-only Data Supplement.

Cell Culture and Blood Outgrowth Endothelial Cell Isolation

Pooled, cryo-preserved primary human umbilical vein endothelial cells (HUVECs) were obtained from Promocell (Heidelberg, Germany) and were cultured as described.[12] Blood outgrowth endothelial cell (BOECs) were isolated as previously described and cultured in EGM-2 medium (Lonza, Basel, Switzerland, CC-3162) supplemented with 18% FCS (Bodinco, Alkmaar, The Netherlands).[12] Experiments were always performed at passage 5 to 6. Venous blood was drawn from an individual with variant MVID, caused by a homozygous 2-bp insertion (c.372_373dup, p.Arg125Leufs*7) in *STX3* (patient 2 in Wiegerinck et al[16]) and from both parents. Blood from an additional variant MVID patient with a homozygous nonsense mutation (c.739C>T, p.Arg247*) in *STX3* (patient 1 in Wiegerinck et al[16]) and the mother of the patient was drawn, but isolation of BOECs was only successful for the heterozygous mother. Control BOECs from healthy donors were isolated from the internal blood donor system at Sanquin Blood Supply. The patient's parents signed an informed consent form for participation. The study was conducted in accordance with the Declaration of Helsinki.

Immunocytochemistry

Endothelial cells were grown on gelatin-coated glass coverslips (Marienfeld, Lauda-Königshofen, Germany). Cells were fixed at room temperature with electron microscopy-grade 4% formaldehyde (Electron Microscopy Sciences, Hatfield) in PBS for 15 minutes followed by simultaneous permeabilization and quenching using 0.2% saponin, 50 mmol/L NH$_4$Cl in PBS. Immunostaining was performed in blocking buffer (PBS, 0.2% gelatin, 0.02% NaN$_3$, and 0.02% saponin). Immunostained cells were mounted in Mowiol 40–88 (Sigma-Aldrich, Steinheim, Germany, 324590), and images were acquired by confocal microscopy using a Leica SP8 (Leica Microsystems, Wetzlar, Germany).

Subcellular Fractionation

HUVECs were grown to confluency, and after 4 days, they were homogenized using a ball-bearing homogenizer (Isobiotec, Heidelberg, Germany) essentially as described previously.[17] Subcellular fractions were obtained by density gradient ultracentrifugation using a Beckmann Optima LX-100 XP ultracentrifuge equipped with a Ti50.2 fixed angle rotor. Briefly, homogenates were fractionated by 2 subsequent Percol (GE Healthcare, Eindhoven, The Netherlands) density gradients followed by 1 Nycodenz (Progen Biotechnik, Heidelberg, Germany) density gradient.[17] Percoll fractions and Nycodenz fractions containing the WPBs were identified by VWF ELISA.[18] Selected fractions were analyzed by immunoblotting for syntaxin-3.

Immunoblotting

Endothelial cells were grown to confluency and lysed in NP-40-based lysis buffer (1% NP-40, 10% glycerol, 1 mmol/L EDTA, 1 mmol/L EGTA, 50 mmol/L Tris HCL, 100 mmol/L NaCL), supplemented with Complete protease inhibitor cocktail (Roche, 05056489001). Proteins were separated on a Novex NuPAGE 4–12% Bis-Tris gel (ThermoFisher, NP0321/NP0323) and transferred onto a nitrocellulose membrane (iBlot Transfer Stack, ThermoFisher, IB3010). Membranes were blocked with Odyssey blocking buffer (LI-COR Biosciences, Lincoln, LI 927) and probed with primary antibodies followed by IRDye-conjugated secondary antibodies. IRDye-conjugated antibodies were visualized by LI-COR Odyssey Infrared Imaging System (LI-COR Biosciences). Image Studio Lite (V4.0, LI-COR Biosciences) was used to analyze band intensities, when needed intensities were normalized to the intensity of α-tubulin which was used as a loading control.

Whole Proteome Analysis of BOECs

BOECs were cultured in 10-cm culture dishes in triplicate. On confluency, cells were rinsed 3× in PBS and subsequently scraped in 100 µL SDS lysis buffer consisting of 4% SDS, 100 mmol/L DTT, 100 mmol/L Tris.HCl pH 7.5, supplemented with MS grade Halt protease and phosphatase inhibitor cocktail (Thermo Scientific, 78440). Next, cell lysates were incubated for 5 minutes at 95°C, sonicated using a Branson Sonifier 250 (Branson Ultrasonics S.A., Geneva, Switzerland), and centrifuged for 10 minutes at 16000g. The cleared lysates were obtained, and the protein concentration was determined by Bradford. Fifty microgram of protein was processed into tryptic peptides using the Filter Aided Sample Preparation method.[19] Ten microgram peptides were desalted and concentrated using Empore-C18 StageTips and eluted with 0.5% (vol/vol) acetic acid and 80% (vol/vol) acetonitrile as described before.[20,21] Sample volume was reduced by SpeedVac and supplemented with 2% (vol/vol) acetonitrile, 0.1% (vol/vol) TFA to a final volume of 5 µL. Three microliter was injected in the Mass Spectrometer (Orbitrap Fusion, Thermo Scientific, Waltham, MA).

Tryptic peptides were separated by nanoscale C18 reverse chromatography coupled online to an Orbitrap Fusion Tribrid mass spectrometer (Thermo Scientific) via a nanoelectrospray ion source (Nanospray Flex Ion Source, Thermo Scientific), using the same settings as described in Gazendam et al.[21] All MS data were acquired with Xcalibur software (Thermo Scientific).

The RAW mass spectrometry files were processed with the MaxQuant computational platform, 1.5.2.8.[22] Proteins and peptides were identified using the Andromeda search engine by querying the human Uniprot database (downloaded February 2015).[23] Standard settings with the additional options match between runs, label-free quantification, and unique peptides for quantification were selected. The generated proteingroups.txt table was filtered for reverse hits, only identified by site and potential contaminants using Perseus 1.5.1.6. The label-free quantification values were transformed in log2 scale. Samples were grouped per BOEC donor (STX3^{−/−} patient, 4 healthy controls; 5 groups, 3 samples per group), and proteins were filtered for at least 3 valid values in at least 1 of the 5 groups. Missing values were imputed by normal distribution (width = 0.3, shift = 1.8), assuming these proteins were close to the detection limit. Global changes in protein levels were assessed using 4 separate volcano plots where the syntaxin-3 patient BOECs were pair-wise compared with the healthy control BOECs (false discovery rate, 0.05, S0: 0.4). Proteins with a significantly changed level were defined as proteins with a significantly changed expression in all 4 pair-wise comparisons.

The.raw MS files and search/identification files obtained with MaxQuant have been deposited in the ProteomeXchange Consortium (http://proteomecentral.proteom exchange.org/cgi/GetDataset) via the PRIDE partner repository,[15] with the data set identifier PXD006176.

Electron Microscopy

BOECs were grown in a petri dish to 5 days post-confluence and were fixed with Karnovsky's fixative followed by 1% osmium-tetroxide post-fixation, en bloc staining with Ultrastain1 (Leica Microsystems), and dehydration by ethanol series. Beem capsules were filled with epon, and the open side of the capsules were positioned on the fixed cells. After polymerization of the EPON, beem capsules were snapped off the surface of the wells of the culture dish. Ultrathin sections (70 nm) parallel to the surface of the beem specimen containing the cultured cells were made on a Reichert Ultracut S (Leica Microsystems). Sections were post-stained with uranylacetate and lead citrate. Electron microscopy images were obtained in a Fei Tecnai Twin transmission electron microscope (FEI, Eindhoven, Netherlands) operating on 120 kV using a Gatan OneView (Gatan, Pleasanton) camera. About 2100 pics per stitch were taken on binning 2. Overlapping images were collected and stitched together into a big image as described.[24] Single WPB images were taken from 7 different cells from stitches of both healthy control BOECs and STX3^{−/−} BOECs (control, n=135; STX3^{−/−}, n=128). All images were randomized after which 6 researchers independently scored the maturation status of all 263 WPB images. Images that were not unanimously recognized as WPBs were excluded (31 from control and 18 from stitch STX3^{−/−}), which led to a final maturity scoring of 104 WPBs from healthy control BOECs and 110 from STX3^{−/−} MVID BOECs.

Secretion Assay

Endothelial cells were grown in 6-well wells or on 24-mm polyester Transwell membranes with 0.4-µm pores (3450, Costar) and cultured at full confluence for 4 to 5 days. Unstimulated VWF release was determined in conditioned EGM-18 medium after 24-hour incubation. Stimulated VWF release was assayed after a 15-minute preincubation in serum-free medium M199 (ThermoFisher, 22340) supplemented with 0.2% (wt/vol) BSA (Merck, 112018). Cells were stimulated in serum-free medium supplemented with 0.1 to 100 µmol/L histamine (Sigma-Aldrich, H7125), 10 µmol/L forskolin (Sigma-Aldrich, F6886) with 100 µmol/L IBMX (Sigma-Aldrich, I7018), or vehicle (unstimulated) for 30 minutes, unless stated otherwise. Lysates were made in serum-free media supplemented with 1% Triton X-100 and protease inhibitors. Polarized VWF secretion was assayed essentially as described,[25] and conditioned media were collected separately from the top (apical) and bottom compartment (basolateral). VWF and VWFpp levels were determined by ELISA.

VWF and VWFpp ELISA

For determination of VWF secretion and intracellular content, a sandwich ELISA was performed using (0.5 µg/well) rabbit polyclonal anti-hVWF (human VWF) as coating antibody and HRP-conjugated rabbit polyclonal anti-hVWF (0.5 µg/mL) for detection. Secreted and intracellular VWFpp was detected by sandwich ELISA using mouse monoclonal anti-hVWFpp (1.0 µg/well) as coating antibody and HRP-conjugated mouse monoclonal anti-hVWFpp (0.125 µg/mL) for detection. Blocking, washing, and detection steps were performed in TWEB buffer (0.1% Tween-20, 0.2% gelatin, and 1 mmol/L EDTA in PBS). HRP activity was measured by colorimetric detection of ortho-phenylenediamine conversion using a Spectramax Plus 384 microplate reader (Molecular Devices, Sunnyvale). Normal plasma from a pool of 30 donors served as a standard for determination of VWF antigen levels in plasma samples.[26] For lysates and media samples, concentrated conditioned media from HEK293Ts (human embryonic kidney 293T cells) stably expressing human wild-type VWF,[27] which was calibrated against the plasma standard, was used as a standard.

DNA Construct and Transfection

For construction of mEGFP (monomeric enhanced green fluorescent protein) tagged to the N-terminus of human STX3, the STX3 coding sequence was amplified with RBNL175 (5′-GGGCGCG CCTGGTGGGGGCCATGAAGGACCGTCTGGAGCAGCTG-3′) and RBNL176 (5′-GCGGCCGCCTGCTCGTCCATTAATTCAGC CCAACGGAAAGTCC-3′) using a human STX3 cDNA clone (clone ID 3010338, Thermo Scientific) as template. The 908 bp polymerase chain reaction product containing the entire STX3 coding sequence was cloned in frame behind mEGFP in the mEGFP-LIC vector by ligation-independent cloning, resulting in mEGFP-STX3. STX3 and VAMP8 were cloned into a lentiviral vector by digestion of the inserts from mEGFP-STX3 using BsrGI and NotI or from pEGFP-VAMP8[28] (a kind gift from Thierry Galli; Addgene No. 42311) using BsrGI and MluI. Fragments were inserted into the previously described LVX-mEGFP-LIC backbone, using the same restriction enzymes, respectively.[12] To construct lentiviral myc-STX3, the 10 residue myc-epitope from myc-LIC[7] was used to replace mEGFP in LVX-mEGFP-LIC through cut and paste cloning with SbfI and BsrGI, resulting in LVX-myc-LIC. STX3 was excised from LVX-mEGFP-STX3 using BsrGI and NotI and cloned in frame behind myc, resulting in LVX-myc-STX3. All constructs were verified by sequence analysis. Transfection of HUVECs was performed by nucleofection as described.[29] Lentivirus was produced in HEK293T cells cultured in EGM-18 as described.[12] Puromycin was used to select for transduced endothelial cells.

Immunoprecipitation

Endothelial cells expressing lentivirally transduced mEGFP-fusion proteins were lysed in lysis buffer (0.5% NP-40, 10 mmol/L Tris. HCl [pH7.5], 150 mmol/L NaCl, and 0.5 mmol/L EDTA) supplemented with Complete Protease Inhibitor Cocktail. Lysates were incubated with magnetic GFP-nanobody beads (Allele Biotech, San Diego; ABP-NAB-GFPM100) or blocked control beads (ABP-NAB-MCNTRL5) by rotation for 2 hours at room temperature. Alternatively, lysates of native HUVECs were lysed and incubated with magnetic protein G dynabeads (Thermo Scientific, 10004D) coupled with antibody as described in the figure. After incubation, beads were washed 4× with lysis buffer. Co-immunoprecipitates and lysates were analyzed by immunoblotting.

CRISPR/Cas9 Engineering of BOECs

gRNAs were designed to exon 1 and exon 2 of the *STX3* gene using the CRISPOR Design tool (http://crispor.tefor.net/crispor. py). gRNAs (gRNA-A exon 1, CTTCAGGATGAAGGACCGTC; gRNA-B exon 2, GACGAGTTCTTTTCTGAGGT) were selected based on the specificity score with the minimum amount of off-target effects and were subsequently cloned as hybridized oligos (gRNA-A: RBNL358 5′-CACCGCTTCAGGATGAAGGACCGTC-3′ and RBNL359 5′-AAACGACGGTCCTTCATCCTGAAGC-3′; gRNA-B:

RBNL364 5′-CACCGGACGAGTTCTTTTCTGAGGT-3′ and RBNL365 5′-AAACACCTCAGAAAAGAACTCGTCC-3′) into BsmBI-digested LentiCRIPSR v2 vector[30] (a kind gift from Feng Zhang; Addgene No. 52961). BOECs were transduced with LentiCRISPR constructs containing gRNA-A or gRNA-B or without gRNA insertion (control) as described above. Puromycin-selected cells were single cell sorted using an antibody against VE-cadherin and plated in 96-well format. Clonal colonies were tested for the expression of syntaxin-3 by immunoblot and STX3 null clones were expanded. To identify the mutations in *STX3*, genomic DNA was isolated using the DNeasy Blood and Tissue kit (QIAGEN, Venlo, NL) from the STX3⁻/⁻ clones. Polymerase chain reaction products amplified using primers for exon 1 (RBNL366: 5′-CGGACGCTCCTCCTAGCTAG-3′ and RBNL367: 5′-GTGGTGAAGGGACCCCTGAC-3′) and exon 2 (RBNL368: 5′-CCCAGCAATTGGTAGAGCTAGG-3′ and RBNL402: 5′-CATG GTTGTGATCCTATGGTTGATTCTG-3′) were subjected to Sanger sequencing and Next Generation Sequencing.

Statistical Analysis

Statistical analysis was by 2-tailed *t* test using GraphPad Prism 7.04 (Graphpad, La Jolla, CA), either paired or unpaired as mentioned in the figure legends. Prior to performing a paired *t* test, normality was confirmed using the Shapiro-Wilk test on small (N=3–6) sample sizes. Prior to performing an unpaired *t* test, normality was approached by a log-transformation, and an *F* test was used to confirm equal variance in larger data sets (N<100). Significance values are shown in the figures or in figure legends. Data are shown as mean±SEM.

Results

The SNARE Protein Syntaxin-3 Is Found on WPBs

In an unbiased proteomic pull down screen for endothelial Slp4-a interaction partners, we have previously identified STXBP1, together with syntaxin-2 and syntaxin-3.[12] Here we determined the intracellular localization of syntaxin-3 in endothelial cells by immunocytochemistry. Endogenous syntaxin-3 immunoreactivity was primarily associated with WPBs in HUVECs (Figure 1A). In an earlier report, Fu et al[11] looked at the cellular distribution of syntaxin-3 in lung microvascular endothelial cells and found that this protein was found primarily at cell–cell contacts and some intracellular punctate structures, but it remained inconclusive whether these represented WPBs. To further test the WPB localization of syntaxin-3, we undertook subcellular fractionation of HUVECs using density gradient ultracentrifugation.[17,18] Consistent with localization on the WPB, syntaxin-3 immunoreactivity cosedimented with VWF in WPB containing subcellular fractions (Figure 1B). This was further confirmed by expression of mEGFP-tagged or myc-tagged syntaxin-3 (Figures I and II in the online-only Data Supplement), which labels WPBs, although interestingly at ectopic expression, a significant proportion was also found on the plasma membrane. Possibly, at normal expression levels, syntaxin-3 is targeted to the WPBs, but at expression levels higher than normal, such as achieved by overexpression of epitope-tagged STX3, this SNARE can also be targeted to alternative locations.

Ex Vivo MVID BOECs Are an Endothelial Deficiency Model for Syntaxin-3

To assess the function of syntaxin-3, we established an ex vivo patient-derived model of syntaxin-3 deficiency using BOECs from an MVID patient with a loss-of-function mutation in *STX3*. MVID is a rare but severe congenital gastrointestinal disorder that manifests itself by chronic diarrhea, malabsorption, metabolic acidosis, and severe dehydration. The abnormal morphology of the enterocytes, which involves microvillus atrophy, intracellular microvillus inclusion bodies, and loss of intestinal epithelial cell polarity, is caused by defective membrane trafficking events as a result of genetic defects in (primarily) *MYO5B* and *STXBP2*.[31,32] Recently, 2 atypical MVID patients have been described with homozygous loss-of-function mutations in *STX3* (Figure 2A).[16] Both patients and several heterozygous, nonaffected family members participated in our study. Table shows the VWF:Ag levels in plasma, which are moderately lower in both patients. BOECs were isolated from peripheral blood mononuclear cells, which was successful for all participants except patient 2. In BOECs from patient 1, who carries a homozygous frame-shifting 2-bp insertion leading to a premature stop (c.372_373dup, p.Arg125Leufs*7) in exon 6 of *STX3*, we were unable to detect syntaxin-3 in its full length or predicted truncated form. BOECs from both heterozygous parents and also the mother of patient 2, who has a heterozygous nonsense mutation leading to a premature stop (c.739C>T, p.Arg247*) in exon 9 of *STX3*, contained ≈50% reduced levels of syntaxin-3 (Figure 2B). This was further confirmed by mass spectrometry analysis of the whole proteome of MVID patient BOECs, which was compared with that of 4 healthy control BOECs (Figure III in the online-only Data Supplement). Interestingly, 5 out of 6 peptides that were found for syntaxin-3 in the healthy control BOECs mapped in the area before the truncation; however, we were unable to accurately detect these in the MVID patient BOECs (not shown). Most probably, both mutations lead to depletion of syntaxin-3 because of either reduced protein stability[16] or nonsense-mediated decay of the mutant transcripts. Consistent with the absence of syntaxin-3 expression, WPBs in BOECs from the MVID patients showed a loss of syntaxin-3 immunoreactivity, while the abundance, distribution, and size of WPBs appeared unaltered (Figure 2C; Figures IV and V in the online-only Data Supplement). CRISPR/Cas9 (clustered regularly interspaced short palindromic repeats/CRISPR-associated 9)-engineered STX3⁻/⁻ BOECs (Figure VI in the online-only Data Supplement) also showed loss of syntaxin-3 immunoreactivity, but like in the patient BOECs, this did not lead to altered morphology of the WPBs (Figure VII in the online-only Data Supplement).

Syntaxin-3 Deficiency Does Not Perturb WPB Formation or Recruitment of Key Membrane Components

SNAREs are key regulators of protein trafficking by facilitating membrane fusion between organelles or during exocytosis. As syntaxin-3, in contrast to syntaxin-4,[11,33] localizes to WPBs rather than the plasma membrane, we investigated whether syntaxin-3 functions in WPB formation and maturation. Throughout its life cycle, the WPB can engage in several membrane fusion steps that contribute to biogenesis, (membrane) content acquisition, or exocytosis.[34] Biogenesis of secretory organelles is generally thought to involve several discrete steps: (1) cargo
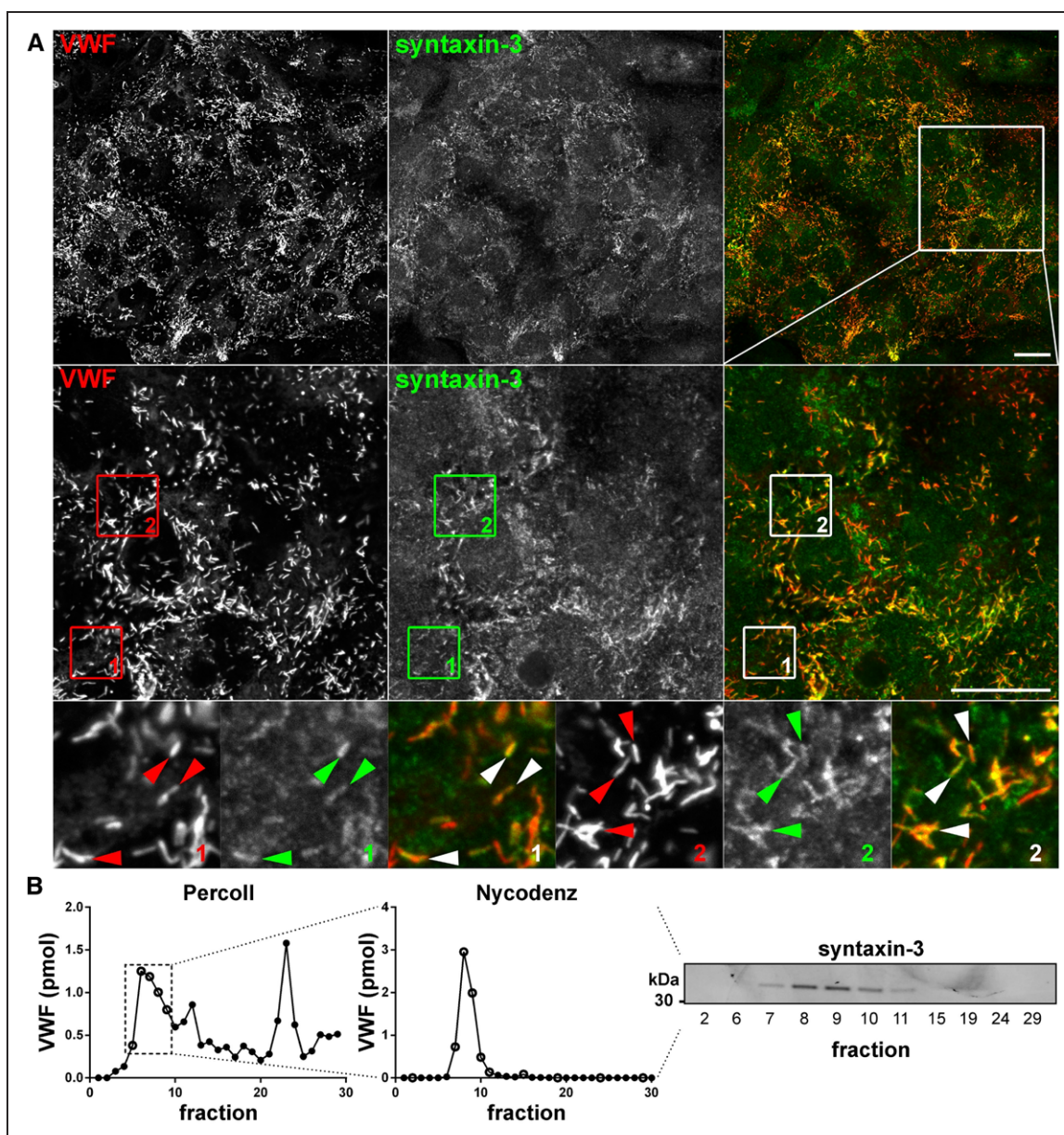
Figure 1. Syntaxin-3 is a Weibel-Palade body (WPB)–associated SNARE (soluble NSF attachment protein receptor). **A**, Human umbilical vein endothelial cells (HUVECs) were immunostained for endogenous von Willebrand factor (VWF; red) and syntaxin-3 (green). Arrowheads indicate syntaxin-3-positive WPBs. Scale bar represents 20 μm. **B**, Subcellular fractionation of HUVECs using density ultracentrifugation. Fractions were assayed for VWF by ELISA to identify WPB containing fractions. Syntaxin-3 presence was assayed using immunoblotting with anti-syntaxin-3 antibodies.

condensation in the trans-Golgi network, (2) budding of nascent/immature secretory granules from the trans-Golgi network, (3) homotypic fusion of immature secretory granules, and (4) removal of excess membrane.[35] To which extent this also applies to WPB biogenesis is still under debate, but there is evidence for the existence of immature WPBs as well as fusion of WPBs.[36–38] We performed ultrastructural analysis of the morphology of large numbers of mature and immature WPBs using transmission electron microscopy stitches of control and STX3−/− BOECs. The numbers and morphometric characteristics of mature WPBs, characterized by intensely condensed cargo, were similar in both wild-type (WT) and STX3−/− samples. When measured, no significant difference in WPB length (WT:

889±335 nm versus STX3−/−: 991±414 nm) but a small, statistically significant difference in width (WT: 173±52 nm versus STX3−/−: 188±61 nm) was observed (Figure 3A through 3D). Immature WPBs, characterized by one or a few discrete VWF tubules loosely surrounded by membrane (Figure 3Aiii and 3Biii), were also found in similar proportions in WT and STX3−/− samples (Figure 3D). WPBs containing hinges (eg, Figure 3Aii and 3Bii) are thought to result from head-on fusion between WPBs.[37] Hinged WPBs were routinely observed in both WT and STX3−/− samples. We also observed normal VWF multimers in plasma from the MVID patient and his parents (Figure 3E; Figure VIII in the online-only Data Supplement), as well as stored in and secreted from cultured STX3−/− BOECs (Figure 3F).
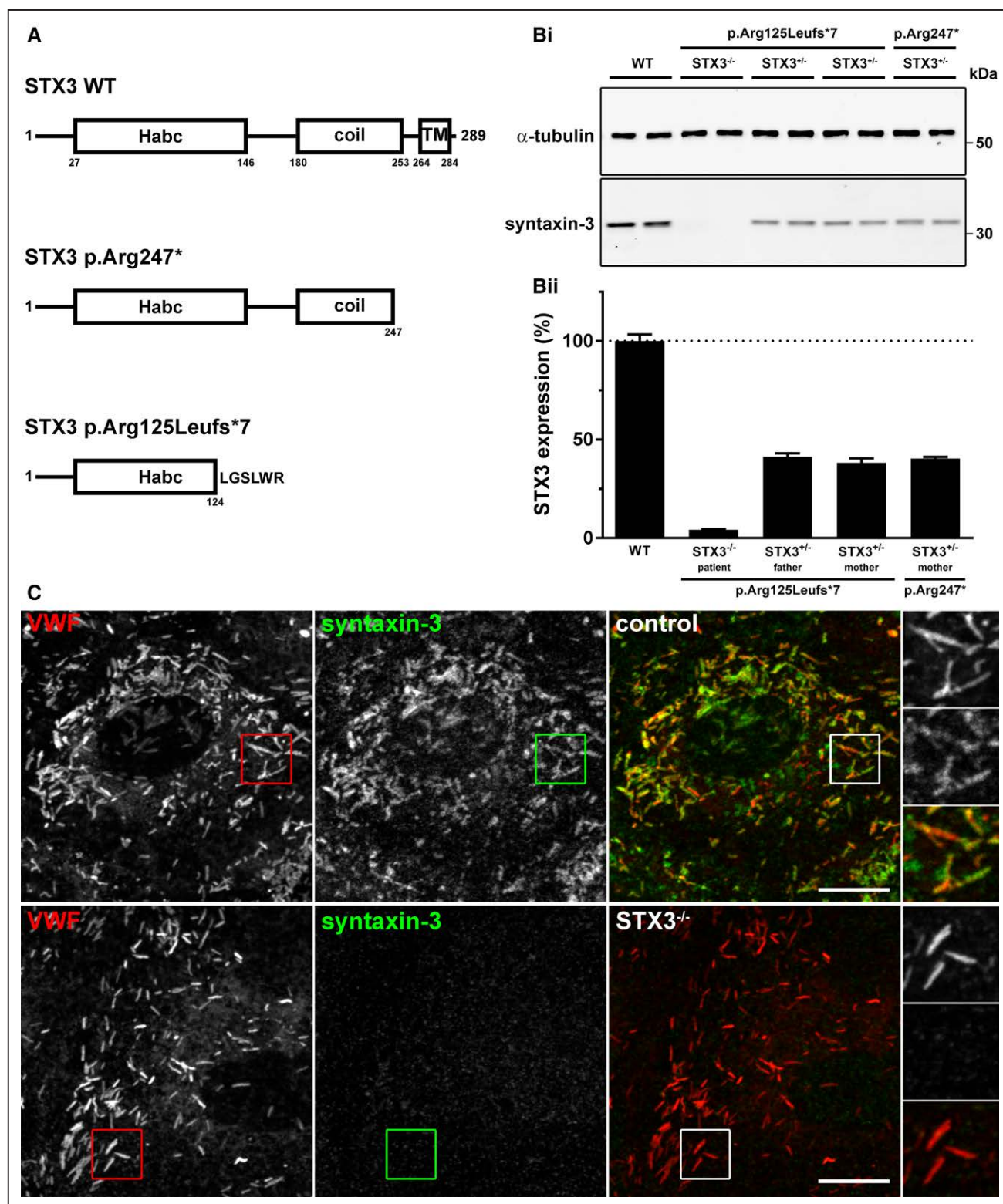
Figure 2. Blood outgrowth endothelial cells (BOECs) from a 2-year-old microvillus inclusion disease (MVID) patient with a homozygous STX3 mutation are devoid of syntaxin-3. **A**, Schematic representation of STX3 domain structure and the predicted patient truncations. p.Arg247* lacks the carboxyterminal transmembrane domain (TM), while p.Arg125Leufs*7 lacks both the TM and the coil domain but includes a 6 residue de novo peptide (LGSLWR) at the carboxyterminus. **Bi**, Healthy control (WT), STX3$^{-/-}$ MVID, and STX3$^{+/-}$ BOEC lysates were separated with SDS-PAGE and were immunoblotted for syntaxin-3; α-tubulin was used as a loading control. **Bii**, Quantification of syntaxin-3 expression in STX3$^{-/-}$ MVID and STX3$^{+/-}$ BOECs normalized to syntaxin-3 in healthy control BOECs (WT). **C**, Healthy control and STX3$^{-/-}$ MVID BOECs were immunostained for von Willebrand factor (VWF; red) and syntaxin-3 (green). Arrowheads point to WPBs. Scale bar represents 10 μm.

Table. Levels of Circulating VWF Measured in MVID Patients and Relatives

Subject	VWF:Ag (IU/mL)
Patient 1 (*STX3*−/−: c.372_373dup, p.Arg125Leufs*7)	0.6
Mother of patient 1 (*STX3*+/−)	2.2
Father of patient 1 (*STX3*+/−)	1.1
Patient 2 (*STX3*−/−: c.739C>T, p.Arg247*)	0.6
Mother of patient 2 (*STX3*+/−)	1.1

MVID indicates microvillus inclusion disease; and VWF, von Willebrand factor.

To determine whether syntaxin-3 plays a role in delivery of key membrane components to the WPB, we first studied the localization of the tetraspanin CD63. The endosome-lysosome marker CD63 is thought to be delivered to WPBs through an AP-3- and annexin-8-dependent interaction/fusion with endosomal compartments.[39–41] Comparison of control and STX3−/− BOECs showed no obvious differences in CD63 localization (Figure 4). In both cases, CD63 was found in abundance in WPBs and also in VWF-negative spherical organelles, most probably representing late endosomes, which in some cases were also syntaxin-3 positive (Figure 4). Localization of the WPB v-SNAREs, VAMP3, and VAMP8[33] (Figure IX in the online-only Data Supplement) and the WPB membrane–associated proteins P-selectin, Rab27A, and Slp4-a (Figures X and XI in the online-only Data Supplement) were also unaffected in STX3−/− BOECs.[3,7,33,42] Taken together, our data suggest that syntaxin-3 does not play a key role in the formation and maturation of WPBs and their content, nor in the recruitment of membrane components to the WPB.

Ex Vivo MVID Endothelial Cells Deficient for Syntaxin-3 Have Impaired Basal and Hormone-Evoked WPB Exocytosis

To investigate the role of syntaxin-3 in WPB exocytosis, we measured hormone-evoked VWF propeptide (VWFpp) release from STX3−/− BOECs. We chose to assay VWFpp because after release from the WPB, VWFpp has a lower retention to the cellular surface than VWF and is therefore a more direct measure of WPB degranulation.[43,44] Intracellular levels of VWFpp were comparable between STX3−/− BOECs and those from a healthy control donor (Figure 5A). However, STX3−/− BOECs showed a significantly reduced release of VWFpp in unstimulated conditions (Figure 5B). Also, STX3−/− BOECs showed a clear stimulus-induced secretion defect: on stimulation with both Ca^{2+}- (histamine) and cAMP-mediated (forskolin) secretagogues, a significant decrease in VWFpp release was observed (Figure 5C), and this was augmented when lower concentrations of histamine were used (Figure 5D). Essentially, similar results were obtained when assaying for secretion of mature VWF (Figure XII in the online-only Data Supplement)

In a recent report it was shown that unstimulated/basal and stimulus-induced VWF secretion are primarily directed toward the endothelial lumen while constitutive secretion of VWF is mostly directed to the basolateral side of the endothelium.[25] To test whether syntaxin-3 contributes to the polarity of VWF secretion, we performed Transwell secretion assays (Figure

XIII in the online-only Data Supplement). Interestingly, while the decrease in stimulated secretion in MVID BOECs is on both sides, the decrease observed in unstimulated VWF secretion was almost entirely caused by a deficit on the apical side (Figure XIIIBi, XIIIBii, XIIICi, and XIIICii in the online-only Data Supplement). Proportionally, while both stimulus-induced and unstimulated VWF release are both released primarily in the apical direction, the polarity of unstimulated release is lost in MVID BOECs (Figure XIIIBiii, XIIIBiv, XIIICiii, and XIIICiv in the online-only Data Supplement). This suggests that syntaxin-3 supports apically directed basal release of WPBs, which during strong activation such as on 100 µmol/L histamine stimulation, can be partially compensated for, possibly by other SNARE complexes.

To study the mechanism by which syntaxin-3 can promote WPB exocytosis, we looked for interactors that have been previously implicated in WPB exocytosis, such as the WPB-associated v-SNAREs VAMP3 and -8 and the t-SNARE SNAP23.[14,33] Co-immunoprecipitation experiments using mEGFP-syntaxin-3 as bait showed that syntaxin-3 predominantly interacts with SNAP23 and VAMP8 and to a lesser extent with VAMP3 (Figure 5E). Similarly, reciprocal pull down using mEGFP-VAMP8 showed coprecipitation of syntaxin-3 but also syntaxin-4 (Figure 5F). This was further confirmed using precipitation of endogenous syntaxin-3 and syntaxin-4 from endothelial cells. VAMP8 and SNAP23 coprecipitated with both endogenous syntaxin-3 and syntaxin-4 (Figure 5G). However, we were unable to confirm endogenous VAMP3 interaction with either syntaxin-3 or syntaxin-4.

Discussion

Circulating levels of VWF are determined by environmental as well as genetic factors, with the heritability of variation being estimated up to 75%.[45–47] In ≈30% of cases, low VWF is caused by mutations outside the *VWF* gene, implying that other genetic loci are involved in regulation of VWF levels.[48] Genome-wide association studies for genetic determinants of VWF levels have identified several new regulators that are suggested to affect secretory processes (*STXBP5* and *STX2*),[13,49] arguing that SNARE-mediated exocytosis of WPBs is a significant determinant of VWF levels. In this study, we have characterized a new component of the WPB regulatory machinery, syntaxin-3, previously identified as a downstream target of the Rab27A–Slp4-a–STXBP1 complex.[12]

The main finding of our study is the identification of SNARE protein syntaxin-3 as a secretory granule localized regulator of WPB exocytosis. The SNARE fusion machinery underlies exocytosis in all secretory cells. Endothelial cells express several members of the SNARE complex, which includes a mixture of t-SNAREs; SNAP23, syntaxin-2, -3, and -4 and WPB-localized v-SNAREs; VAMP3 and VAMP8.[11,12,14,33] The SNARE complexes formed are in turn regulated by SNARE-associated proteins, including STXBP1, STXBP3, and STXBP5.[11–13] However, the precise number and composition of SNARE complexe(s) and their specific roles in controlling VWF secretion remains unclear. In the context of such a complex cocktail of SNAREs, it can prove challenging to single out the contribution of an individual component, especially because residual levels of SNAREs that remain on
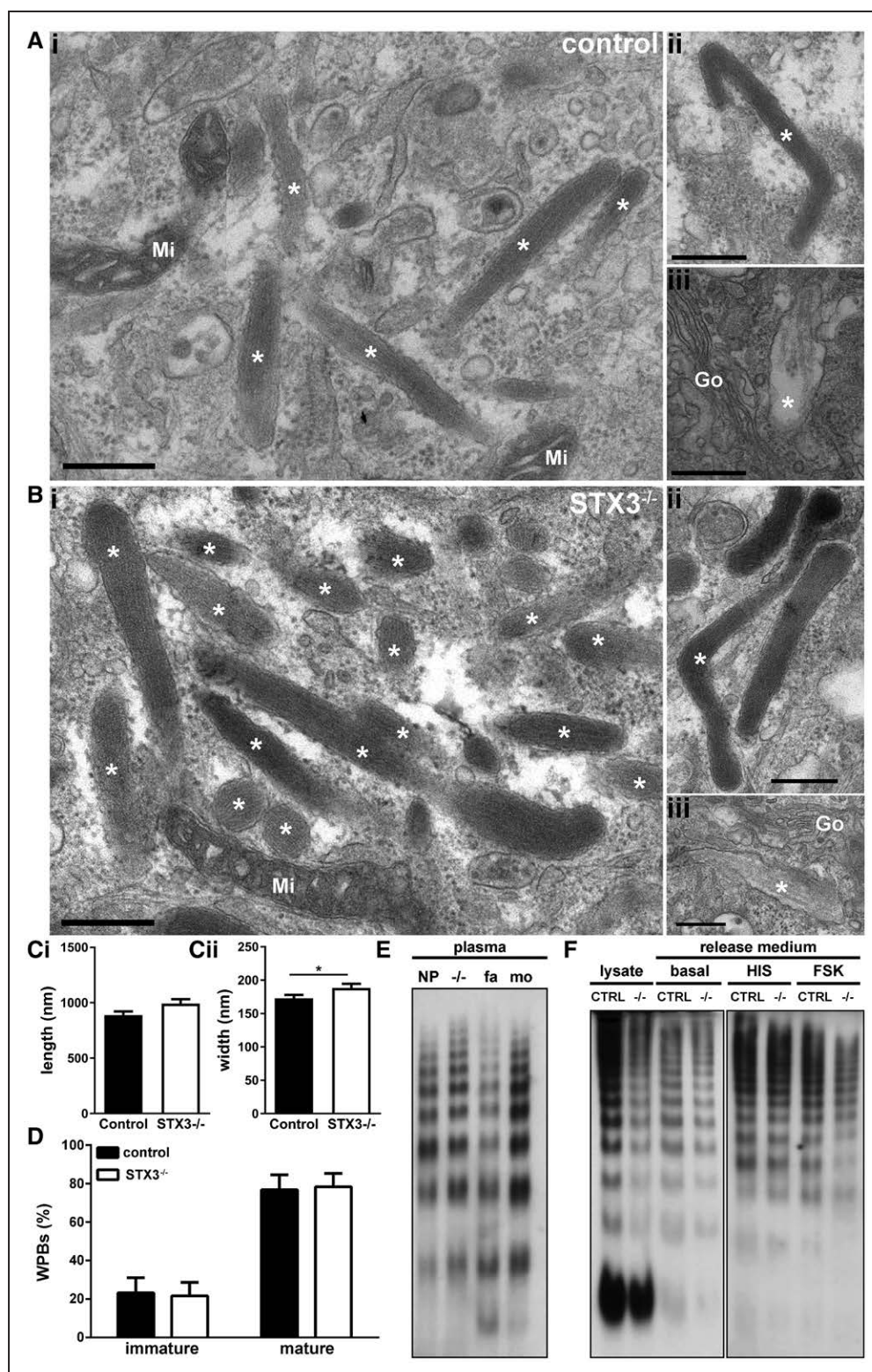
Figure 3. Syntaxin-3 deficiency does not affect Weibel-Palade body (WPB) maturation. **A–D,** Healthy control blood outgrowth endothelial cells (BOECs; **A**) and STX3^{−/−} BOECs (**B**) were cultured at full confluency for 4 to 5 days before fixation for electron microscopy (EM) stitches. **A** and **B,** Representative images taken from EM stitches showing grouped WPBs (**i**), hinged WPBs (**ii**), and immature WPBs (**iii**), indicated with asterisks. Scale bars represent 400 nm. **C** and **D,** Images of single WPBs were taken from healthy control (n=104) and STX3^{−/−} (n=110) EM stitch images. Length and width were measured (**C**), and WPB maturity was scored by 6 individuals (**D**). Statistical analysis was performed using a 2-tailed *t* test on log-transformed values to approach normal distribution. Error bars represent SEM. *$P<0.05$. **E,** Multimer analysis of von Willebrand factor (VWF) in plasma samples taken from a STX3^{−/−} microvillus inclusion disease (MVID) patient (−/−) and his STX3^{+/−} father (fa) and mother (mo) compared with pooled normal plasma (NP). **F,** Multimer analysis of VWF in lysates and release medium of healthy control (**C**) and STX3^{−/−} BOECs (−/−). Release medium was taken after 24 hours without stimulation (basal) or after 30 minutes of stimulation with 100 mmol/L histamine (HIS) or 10 μmol/L forskolin+100 μmol/L IBMX (FSK). Go indicates Golgi; and Mi, mitochondrium.
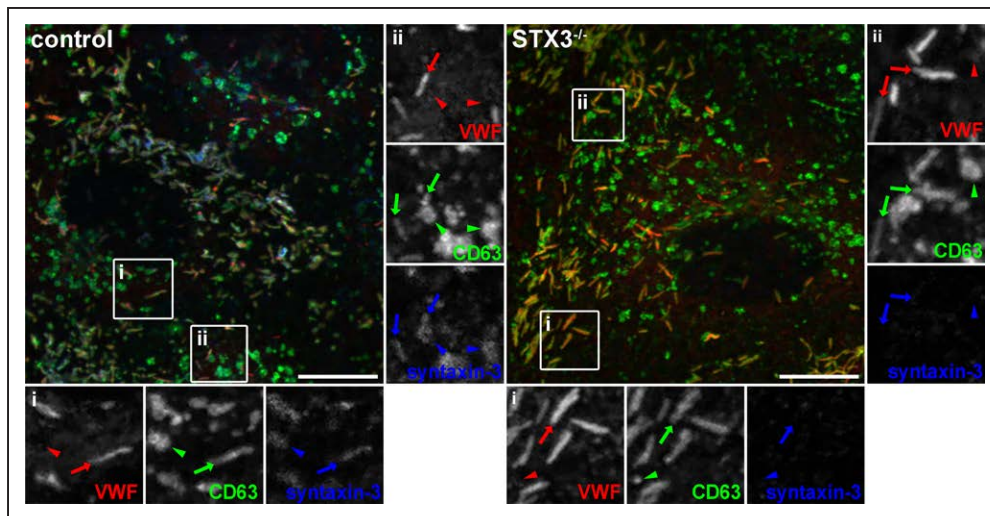
Figure 4. Weibel-Palade body (WPB) targeting of CD63 is not dependent on syntaxin-3. Healthy control (control) and STX3^{-/-} microvillus inclusion disease (MVID; STX3^{-/-}) blood outgrowth endothelial cell (BOECs) were grown at full confluence for 5 to 7 days before fixation. Cells were immunostained with mouse IgG2b-CD63 (green), mouse IgG1 anti-von Willebrand factor (VWF; red), and rabbit anti-syntaxin-3 (blue). Arrows indicate WPBs that are positive for CD63 and in the control cells also for syntaxin-3. Arrowheads indicate potential endosomes positive for CD63 and in the control cells also syntaxin-3. Scale bars are 10 μm.

depletion using RNA interference have been reported to suffice for their function.[50] Therefore, we took the opportunity to study the role of syntaxin-3 in a patient-derived endothelial model of complete syntaxin-3 deficiency using BOECs from an MVID patient with mutations in *STX3*. Our results show that complete loss of syntaxin-3 leads to a significant attenuation of VWFpp and VWF secretion.

In syntaxin-3-deficient MVID patients, circulating levels of VWF are at the low end of the normal range for the general population, although not associated with bleeding complications. Plasma levels of VWF are thought to be maintained by unstimulated VWF secretion by the endothelium, which arises primarily from basal release of WPBs.[25,51] In line with this, analysis of STX3^{-/-} BOECs showed a small but statistically significant reduction in unstimulated VWF and VWFpp secretion (Figure 5B). There was also clear defect of stimulus-induced secretion in STX3^{-/-} BOECs: we observed a significant reduction of VWFpp and VWF secretion on challenging with Ca^{2+}- or cAMP-mediated secretagogues. However, WPB release was not completely abolished, which most likely reflects functional redundancy through syntaxin-3-independent SNARE complexes that are able to partially compensate for the loss of syntaxin-3. Because VWF secretion from the endothelium is such a critically important process, as illustrated by patients with type III Von Willebrand disease, a high degree of redundancy in the molecular regulation of VWF secretion may reflect an evolutionary drive to maintain this vital process. Indeed, of the SNARE-(associated) mediators of WPB release identified to date, the consequence of depletion of any one factor leads, in the majority of cases, to only a partial reduction of stimulated WPB release.[7,11,12,14,33] This may also explain why genetic disorders affecting a single component of the WPB exocytosis machinery are often not accompanied by significant hemostatic complications or why genetic variations such as identified in genome-wide association studies studies

are associated with modest effects on VWF levels.[52–54] Using several distinct SNARE complexes potentially also enables the endothelium to have greater control over its secretory response (eg, release of different subsets of WPBs), support different modes of exocytosis, or control release at specific sites. Attempts to experimentally rescue the secretory defect in STX3-deficient BOECs using ectopically expressed STX3 were unsuccessful and even attenuated stimulated VWF release in both STX3^{-/-} and control BOECs (data not shown), possibly because of mistargeting of a pool of epitope-tagged STX3 (Figures I and II in the online-only Data Supplement). Whether this was the result of the epitope-tag or the inability to experimentally control the ectopic expression levels remains unclear, but this may be further indication that the proper function of syntaxin-3 in WPB exocytosis depends on its localization on the secretory vesicle.

MVID is characterized by a failure of enterocytes, polarized intestinal epithelial cells, to target microvilli to their apical surface. This manifests as a loss of brush-border microvilli, basolateral targeting of microvilli, and the formation of microvillus inclusion bodies. Syntaxin-3, which contains an N-terminal apical targeting motif, is normally found at the apical side where it supports delivery of apical membrane proteins involved in the formation of microvilli. Loss of syntaxin-3, such as in the MVID patient from whom we established STX3^{-/-} BOECs, leads to a loss of polarity and mistargeting of apical cargo to the basolateral side where syntaxin-4 is found.[16,55–57] Endothelial cells also exhibit apical/basolateral polarity with the apical side facing the vessel lumen, while the basolateral side is connected to the subendothelial matrix. Recently, evidence has been presented that endothelial cells secrete high molecular weight VWF from a stored WPB pool predominantly at the apical side, where it is ideally positioned to support platelet adherence. In contrast, low molecular weight VWF is secreted constitutively at the basolateral side.[25] The mechanisms that dictate this preference
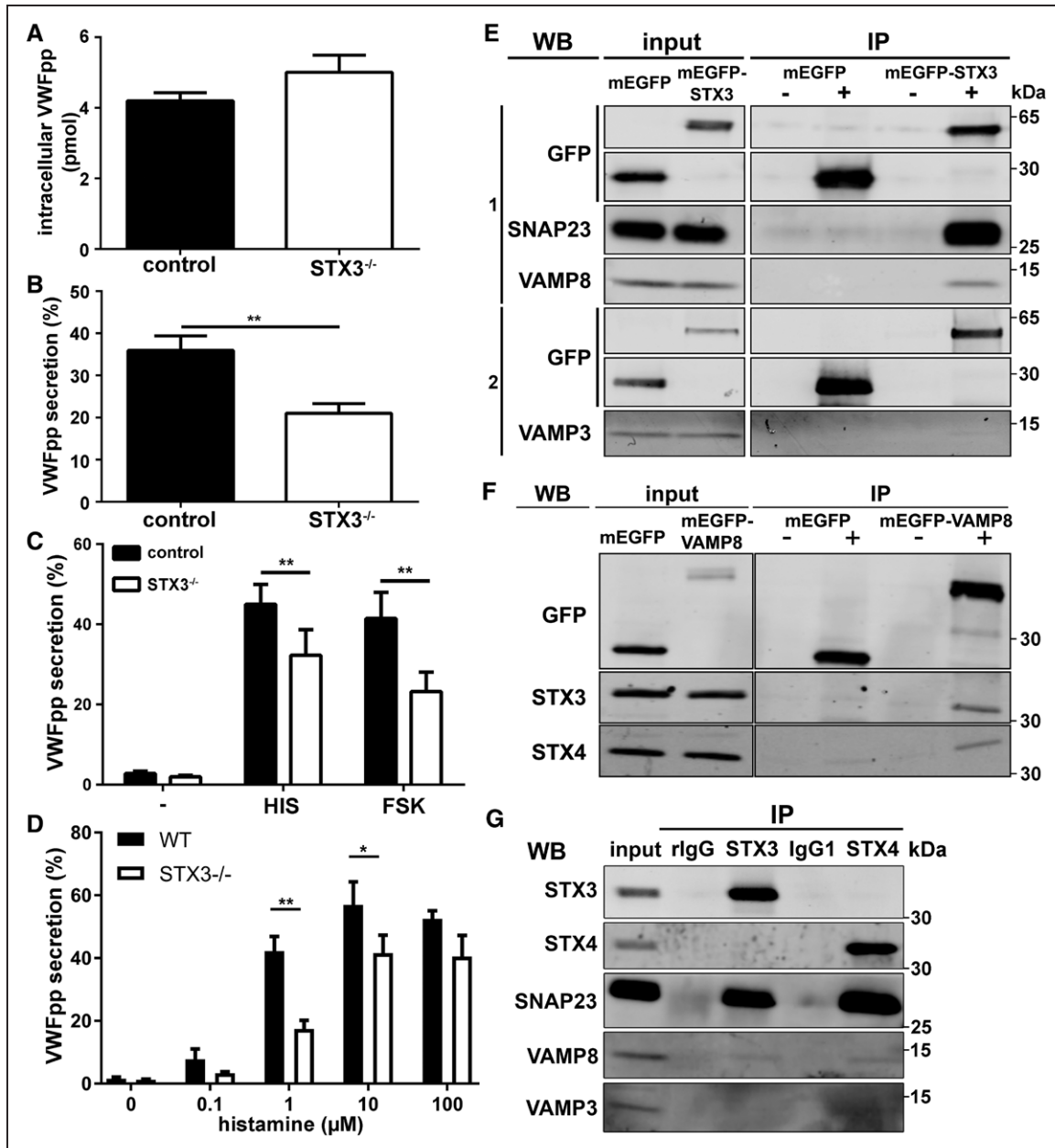
Figure 5. VWFpp release is impaired in STX3$^{-/-}$ microvillus inclusion disease (MVID) blood outgrowth endothelial cell (BOECs). **A**, Intracellular VWFpp levels in healthy control and STX3$^{-/-}$ MVID BOECs (n=6). **B**, VWFpp levels in 24 hours conditioned medium from control and STX3$^{-/-}$ BOECs (n=6). **C**, VWFpp release from control and STX3$^{-/-}$ BOECs after 30 minute stimulation with 100 μmol/L histamine (HIS) or 10 μmol/L forskolin+100 μmol/L IBMX (FSK). Release of VWFpp is expressed as percentage of intracellular VWFpp (n=6). **D**, Dose dependency of histamine-stimulated VWFpp release from control and STX3$^{-/-}$ BOECs (n=3). Statistical analyses were performed using paired 2-tailed *t* tests (**A**–**D**). Error bars represent SEM. *$P<0.05$ **$P<0.01$. **E** and **F**, Lysates of endothelial cells expressing mEGFP (monomeric enhanced green fluorescent protein), mEGFP-STX3 (**E**) or mEGFP-VAMP8 (vesicle-associated membrane protein-8; **F**) were incubated with magnetic beads covalently coupled with anti-GFP nanobody (+) or control beads (−). **G**, Human umbilical vein endothelial cell (HUVEC) lysates were incubated with magnetic beads covalently coupled with rabbit anti-syntaxin-3 IgG or an equivalent amount of naive rabbit IgG and with mouse anti-syntaxin-4 IgG1 or an equivalent amount of naive mouse IgG1. Immunoblots of lysates (input) and co-immunoprecipitates (IP) were probed with anti-GFP, anti-SNAP23, anti-VAMP8, anti-VAMP3, anti-syntaxin-3 (STX3), or anti syntaxin-4 (STX4; **E**–**G**).

for the apical side are still unknown, but our data suggest that syntaxin-3 supports apical release of WPBs.

Membrane fusion events in the regulated secretory pathway can be heterotypic (fusion between different compartments, ie, WPB–plasma membrane) or homotypic (fusion of similar intracellular compartments, eg, WPB–WPB). One previously described homotypic fusion mode is compound fusion, in which several WPBs fuse intracellularly prior to

exocytosis. Upon compound fusion, enlarged, rounded structures are formed, termed secretory pods, that contain disordered VWF tubules.[58,59] A related but distinct mode of WPB fusion, termed sequential or cumulative exocytosis, has recently been reported.[60,61] In this mode, a post-fusion WPB provides a membrane site for subsequent cumulative fusion of additional WPBs. The mechanisms underlying homotypic WPB fusion are not known; however, in mast and pancreatic

acinar cells, cumulative fusion is the predominant form of exocytosis and has been studied more extensively. In both cell types, syntaxin-3 is found on the secretory organelles.[62,63] In acinar cells, syntaxin-3 was found to pair with SNAP23 and VAMP8, the latter of which is also found on WPBs, while syntaxin-2 complexed with VAMP2 and SNAP23. During sequential exocytosis, syntaxin-2 and syntaxin-3 containing SNARE machineries were found to support distinct steps: primary granules were released via syntaxin-2, while the subsequent secondary steps were dependent on syntaxin-3.[64] A similar mechanism was described in insulin granule exocytosis from pancreatic beta cells, where syntaxin-3 regulates exocytosis of a secondary, newcomer granule.[65] One difference between compound and cumulative fusion is the strength of stimulus required to set these pathways in motion: in eosinophils compound fusion becomes more prevalent in conditions of high stimulus, while the incidence of cumulative fusion is increased at low levels of stimulus.[66] In that respect, it is noteworthy that at lower concentration of histamine, the loss of syntaxin-3 leads to a more prominent decrease in VWFpp secretion (Figure 5D; Figure XIID in the online-only Data Supplement).

Taken together, our data identify syntaxin-3 as a novel WPB-localized regulator of VWF secretion which, depending on the degree of endothelial activation, takes a prominent role in WPB release at the apical side of endothelial cells. Based on its interactions with (WPB-localized) SNAREs that have been previously implicated in VWF secretion, we speculate that a homotypic fusion mode of WPBs is the underlying mechanisms by which syntaxin-3 facilitates exocytosis (Figure 6). Future studies should address whether assembly of *trans*-complexes of t-SNAREs and v-SNAREs on opposing WPBs contribute to homotypic fusion modes, such as compound or sequential/cumulative fusion.
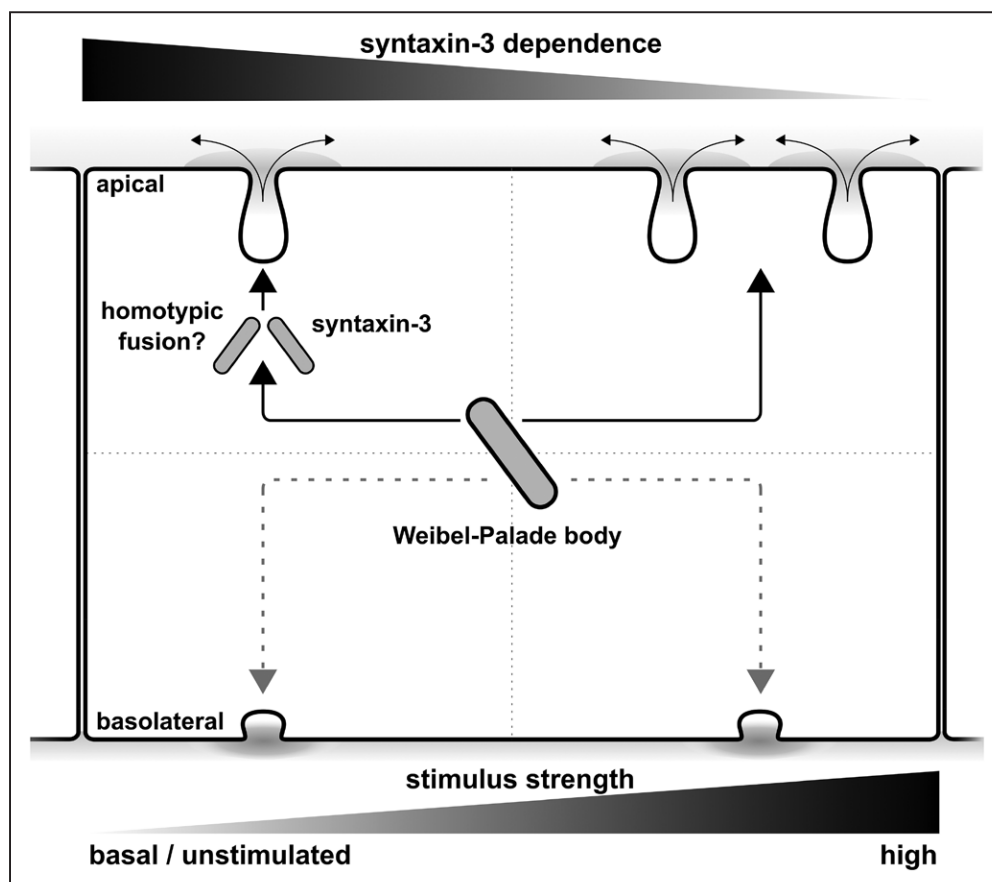
Acknowledgments

Sources of Funding

Figure 6. Proposed model of syntaxin-3 function in Weibel-Palade body (WPB) exocytosis. Cartoon representation of a WPB undergoing polarized release as a function of stimulus intensity. Depending on the strength of stimulus, WPBs can undergo syntaxin-3-dependent and -independent release, both of which occur primarily at the apical face of endothelial cells (Figure XIII in the online-only Data Supplement). During conditions of low concentration secretagogue stimulus or during basal release, WPBs use a syntaxin-3 dependent pathway, possibly by an exocytotic mode that involves homotypic fusion of WPBs through SNARE (soluble NSF attachment protein receptor) pairing of syntaxin-3 with v-SNARE VAMP8 at opposing WPBs (Figure 5E through 5G), which is primarily directed to the apical side of the endothelium. At elevated levels of endothelial activation, the inhibition of (polarized) von Willebrand factor (VWF) secretion in the absence of syntaxin-3 is (partly) overcome (Figure 5; Figure XIII in the online-only Data Supplement) because of the increasing contribution of syntaxin-3-independent pathways that are able to compensate for the loss of syntaxin-3.

Disclosures

None.

References

1. Sadler JE. von Willebrand factor: two sides of a coin. *J Thromb Haemost*. 2005;3:1702–1709. doi: 10.1111/j.1538-7836.2005.01369.x.

2. Rondaij MG, Bierings R, Kragt A, van Mourik JA, Voorberg J. Dynamics and plasticity of Weibel-Palade bodies in endothelial cells. *Arterioscler Thromb Vasc Biol*. 2006;26:1002–1007. doi: 10.1161/01.ATV.0000209501.56852.6c.

3. Hannah MJ, Hume AN, Arribas M, Williams R, Hewlett LJ, Seabra MC, Cutler DF. Weibel-Palade bodies recruit Rab27 by a content-driven, maturation-dependent mechanism that is independent of cell type. *J Cell Sci*. 2003;116(pt 19):3939–3948. doi: 10.1242/jcs.00711.

4. Knop M, Aareskjold E, Bode G, Gerke V. Rab3D and annexin A2 play a role in regulated secretion of vWF, but not tPA, from endothelial cells. *EMBO J*. 2004;23:2982–2992. doi: 10.1038/sj.emboj.7600319.

5. Nightingale TD, Pattni K, Hume AN, Seabra MC, Cutler DF. Rab27a and MyRIP regulate the amount and multimeric state of VWF released from endothelial cells. *Blood*. 2009;113:5010–5018. doi: 10.1182/blood-2008-09-181206.

6. Rojo Pulido I, Nightingale TD, Darchen F, Seabra MC, Cutler DF, Gerke V. Myosin Va acts in concert with Rab27a and MyRIP to regulate acute von-Willebrand factor release from endothelial cells. *Traffic*. 2011;12:1371–1382. doi: 10.1111/j.1600-0854.2011.01248.x.

7. Bierings R, Hellen N, Kiskin N, Knipe L, Fonseca AV, Patel B, Meli A, Rose M, Hannah MJ, Carter T. The interplay between the Rab27A effectors Slp4-a and MyRIP controls hormone-evoked Weibel-Palade body exocytosis. *Blood*. 2012;120:2757–2767. doi: 10.1182/blood-2012-05-429936.

8. Zografou S, Basagiannis D, Papafotika A, Shirakawa R, Horiuchi H, Auerbach D, Fukuda M, Christoforidis S. A complete Rab screening reveals novel insights in Weibel-Palade body exocytosis. *J Cell Sci*. 2012;125(pt 20):4780–4790. doi: 10.1242/jcs.104174.

9. Conte IL, Hellen N, Bierings R, Mashanov GI, Manneville JB, Kiskin NI, Hannah MJ, Molloy JE, Carter T. Interaction between MyRIP and the actin cytoskeleton regulates Weibel-Palade body trafficking and exocytosis. *J Cell Sci*. 2016;129:592–603. doi: 10.1242/jcs.178285.

10. Matsushita K, Morrell CN, Cambien B, Yang SX, Yamakuchi M, Bao C, Hara MR, Quick RA, Cao W, O'Rourke B, Lowenstein JM, Pevsner J, Wagner DD, Lowenstein CJ. Nitric oxide regulates exocytosis by S-nitrosylation of N-ethylmaleimide-sensitive factor. *Cell*. 2003;115:139–150.

11. Fu J, Naren AP, Gao X, Ahmmed GU, Malik AB. Protease-activated receptor-1 activation of endothelial cells induces protein kinase Calpha-dependent phosphorylation of syntaxin 4 and Munc18c: role in signaling p-selectin expression. *J Biol Chem*. 2005;280:3178–3184. doi: 10.1074/jbc.M410044200.

12. van Breevoort D, Snijders AP, Hellen N, Weckhuysen S, van Hooren KW, Eikenboom J, Valentijn K, Fernandez-Borja M, Ceulemans B, De Jonghe P, Voorberg J, Hannah M, Carter T, Bierings R. STXBP1 promotes Weibel-Palade body exocytosis through its interaction with the Rab27A effector Slp4-a. *Blood*. 2014;123:3185–3194. doi: 10.1182/blood-2013-10-535831.

13. Zhu Q, Yamakuchi M, Ture S, de la Luz Garcia-Hernandez M, Ko KA, Modjeski KL, LoMonaco MB, Johnson AD, O'Donnell CJ, Takai Y, Morrell CN, Lowenstein CJ. Syntaxin-binding protein STXBP5 inhibits endothelial exocytosis and promotes platelet secretion. *J Clin Invest*. 2014;124:4503–4516. doi: 10.1172/JCI71245.

14. Zhu Q, Zhu Q, Yamakuchi M, Lowenstein CJ. SNAP23 regulates endothelial exocytosis of von Willebrand Factor. *PLoS One*. 2015;10:e0118737. doi: 10.1371/journal.pone.0118737.

15. Vizcaíno JA, Deutsch EW, Wang R, et al. ProteomeXchange provides globally coordinated proteomics data submission and dissemination. *Nat Biotechnol*. 2014;32:223–226. doi: 10.1038/nbt.2839.

16. Wiegerinck CL, Janecke AR, Schneeberger K, et al. Loss of syntaxin 3 causes variant microvillus inclusion disease. *Gastroenterology*. 2014;147:65–68.e10. doi: 10.1053/j.gastro.2014.04.002.

17. van Breevoort D, van Agtmaal EL, Dragt BS, Gebbinck JK, Dienava-Verdoold I, Kragt A, Bierings R, Horrevoets AJ, Valentijn KM,

18. Bierings R, van den Biggelaar M, Kragt A, Mertens K, Voorberg J, van Mourik JA. Efficiency of von Willebrand factor-mediated targeting of interleukin-8 into Weibel-Palade bodies. *J Thromb Haemost*. 2007;5:2512–2519. doi: 10.1111/j.1538-7836.2007.02768.x.

19. Wiśniewski JR, Zougman A, Nagaraj N, Mann M. Universal sample preparation method for proteome analysis. *Nat Methods*. 2009;6:359–362. doi: 10.1038/nmeth.1322.

20. Rappsilber J, Ishihama Y, Mann M. Stop and go extraction tips for matrix-assisted laser desorption/ionization, nanoelectrospray, and LC/MS sample pretreatment in proteomics. *Anal Chem*. 2003;75:663–670.

21. Gazendam RP, van de Geer A, van Hamme JL, Tool AT, van Rees DJ, Aarts CE, van den Biggelaar M, van Alphen F, Verkuijlen P, Meijer AB, Janssen H, Roos D, van den Berg TK, Kuijpers TW. Impaired killing of Candida albicans by granulocytes mobilized for transfusion purposes: a role for granule components. *Haematologica*. 2016;101:587–596. doi: 10.3324/haematol.2015.136630.

22. Cox J, Mann M. MaxQuant enables high peptide identification rates, individualized p.p.b.-range mass accuracies and proteome-wide protein quantification. *Nat Biotechnol*. 2008;26:1367–1372. doi: 10.1038/nbt.1511.

23. Bateman A, Martin MJ, O'Donovan C, et al. UniProt: a hub for protein information. *Nucleic Acids Res*. 2015;43:D204–D212.

24. Faas FG, Avramut MC, van den Berg BM, Mommaas AM, Koster AJ, Ravelli RB. Virtual nanoscopy: generation of ultra-large high resolution electron microscopy maps. *J Cell Biol*. 2012;198:457–469. doi: 10.1083/jcb.201201140.

25. Lopes da Silva M, Cutler DF. von Willebrand factor multimerization and the polarity of secretory pathways in endothelial cells. *Blood*. 2016;128:277–285.

26. van Mourik JA, Boertjes R, Huisveld IA, Fijnvandraat K, Pajkrt D, van Genderen PJ, Fijnheer R. von Willebrand factor propeptide in vascular disorders: A tool to distinguish between acute and chronic endothelial cell perturbation. *Blood*. 1999;94:179–185.

27. van den Biggelaar M, Bierings R, Storm G, Voorberg J, Mertens K. Requirements for cellular co-trafficking of factor VIII and von Willebrand factor to Weibel-Palade bodies. *J Thromb Haemost*. 2007;5:2235–2242. doi: 10.1111/j.1538-7836.2007.02737.x.

28. Paumet F, Le Mao J, Martin S, Galli T, David B, Blank U, Roa M. Soluble NSF attachment protein receptors (SNAREs) in RBL-2H3 mast cells: functional role of syntaxin 4 in exocytosis and identification of a vesicle-associated membrane protein 8-containing secretory compartment. *J Immunol*. 2000;164:5850–5857.

29. Knipe L, Meli A, Hewlett L, Bierings R, Dempster J, Skehel P, Hannah MJ, Carter T. A revised model for the secretion of tPA and cytokines from cultured endothelial cells. *Blood*. 2010;116:2183–2191. doi: 10.1182/blood-2010-03-276170.

30. Sanjana NE, Shalem O, Zhang F. Improved vectors and genome-wide libraries for CRISPR screening. *Nat Methods*. 2014;11:783–784. doi: 10.1038/nmeth.3047.

31. Müller T, Hess MW, Schiefermeier N, et al. MYO5B mutations cause microvillus inclusion disease and disrupt epithelial cell polarity. *Nat Genet*. 2008;40:1163–1165. doi: 10.1038/ng.225.

32. Stepensky P, Bartram J, Barth TF, Lehmberg K, Walther P, Amann K, Philips AD, Beringer O, Zur Stadt U, Schulz A, Amrolia P, Weintraub M, Debatin KM, Hoenig M, Posovszky C. Persistent defective membrane trafficking in epithelial cells of patients with familial hemophagocytic lymphohistiocytosis type 5 due to STXBP2/MUNC18-2 mutations. *Pediatr Blood Cancer*. 2013;60:1215–1222. doi: 10.1002/pbc.24475.

33. Pulido IR, Jahn R, Gerke V. VAMP3 is associated with endothelial weibel-palade bodies and participates in their Ca(2+)-dependent exocytosis. *Biochim Biophys Acta*. 2011;1813:1038–1044. doi: 10.1016/j.bbamcr.2010.11.007.

34. Valentijn KM, Sadler JE, Valentijn JA, Voorberg J, Eikenboom J. Functional architecture of Weibel-Palade bodies. *Blood*. 2011;117:5033–5043. doi: 10.1182/blood-2010-09-267492.

35. Tooze SA, Martens GJ, Huttner WB. Secretory granule biogenesis: rafting to the SNARE. *Trends Cell Biol*. 2001;11:116–122.

36. Zenner HL, Collinson LM, Michaux G, Cutler DF. High-pressure freezing provides insights into Weibel-Palade body biogenesis. *J Cell Sci*. 2007;120(pt 12):2117–2125. doi: 10.1242/jcs.007781.

37. Valentijn KM, Valentijn JA, Jansen KA, Koster AJ. A new look at Weibel-Palade body structure in endothelial cells using electron tomography. *J Struct Biol*. 2008;161:447–458. doi: 10.1016/j.jsb.2007.08.001.

38. Ferraro F, Kriston-Vizi J, Metcalf DJ, Martin-Martin B, Freeman J, Burden JJ, Westmoreland D, Dyer CE, Knight AE, Ketteler R, Cutler DF. A two-tier Golgi-based control of organelle size underpins the functional plasticity of endothelial cells. *Dev Cell*. 2014;29:292–304. doi: 10.1016/j.devcel.2014.03.021.

39. Kobayashi T, Vischer UM, Rosnoblet C, Lebrand C, Lindsay M, Parton RG, Kruithof EK, Gruenberg J. The tetraspanin CD63/lamp3 cycles between endocytic and secretory compartments in human endothelial cells. *Mol Biol Cell*. 2000;11:1829–1843.

40. Harrison-Lavoie KJ, Michaux G, Hewlett L, Kaur J, Hannah MJ, Lui-Roberts WW, Norman KE, Cutler DF. P-selectin and CD63 use different mechanisms for delivery to Weibel-Palade bodies. *Traffic*. 2006;7:647–662. doi: 10.1111/j.1600-0854.2006.00415.x.

41. Poeter M, Brandherm I, Rossaint J, Rosso G, Shahin V, Skryabin BV, Zarbock A, Gerke V, Rescher U. Annexin A8 controls leukocyte recruitment to activated endothelial cells via cell surface delivery of CD63. *Nat Commun*. 2014;5:3738. doi: 10.1038/ncomms4738.

42. McEver RP, Beckstead JH, Moore KL, Marshall-Carlson L, Bainton DF. GMP-140, a platelet alpha-granule membrane protein, is also synthesized by vascular endothelial cells and is localized in Weibel-Palade bodies. *J Clin Invest*. 1989;84:92–99. doi: 10.1172/JCI114175.

43. Hannah MJ, Skehel P, Erent M, Knipe L, Ogden D, Carter T. Differential kinetics of cell surface loss of von Willebrand factor and its propolypeptide after secretion from Weibel-Palade bodies in living human endothelial cells. *J Biol Chem*. 2005;280:22827–22830. doi: 10.1074/jbc.M412547200.

44. Hewlett L, Zupančič G, Mashanov G, Knipe L, Ogden D, Hannah MJ, Carter T. Temperature-dependence of Weibel-Palade body exocytosis and cell surface dispersal of von Willebrand factor and its propolypeptide. *PLoS One*. 2011;6:e27314. doi: 10.1371/journal.pone.0027314.

45. de Lange M, Snieder H, Ariëns RA, Spector TD, Grant PJ. The genetics of haemostasis: a twin study. *Lancet*. 2001;357:101–105. doi: 10.1016/S0140-6736(00)03541-8.

46. Bladbjerg EM, de Maat MP, Christensen K, Bathum L, Jespersen J, Hjelmborg J. Genetic influence on thrombotic risk markers in the elderly–a Danish twin study. *J Thromb Haemost*. 2006;4:599–607. doi: 10.1111/j.1538-7836.2005.01778.x.

47. Desch KC, Ozel AB, Siemieniak D, et al. Linkage analysis identifies a locus for plasma von Willebrand factor undetected by genome-wide association. *Proc Natl Acad Sci U S A*. 2013;110:588–593. doi: 10.1073/pnas.1219885110.

48. Leebeek FW, Eikenboom JC. Von Willebrand's Disease. *N Engl J Med*. 2016;375:2067–2080. doi: 10.1056/NEJMra1601561.

49. Smith NL, Chen MH, Dehghan A, et al.; Wellcome Trust Case Control Consortium;. Novel associations of multiple genetic loci with plasma levels of factor VII, factor VIII, and von Willebrand factor: The CHARGE (Cohorts for Heart and Aging Research in Genome Epidemiology) Consortium. *Circulation*. 2010;121:1382–1392. doi: 10.1161/CIRCULATIONAHA.109.869156.

50. Bethani I, Werner A, Kadian C, Geumann U, Jahn R, Rizzoli SO. Endosomal fusion upon SNARE knockdown is maintained by residual SNARE activity and enhanced docking. *Traffic*. 2009;10:1543–1559. doi: 10.1111/j.1600-0854.2009.00959.x.

51. Giblin JP, Hewlett LJ, Hannah MJ. Basal secretion of von Willebrand factor from human endothelial cells. *Blood*. 2008;112:957–964. doi: 10.1182/blood-2007-12-130740.

52. Van Gele M, Dynoodt P, Lambert J. Griscelli syndrome: a model system to study vesicular trafficking. *Pigment Cell Melanoma Res*. 2009;22:268–282. doi: 10.1111/j.1755-148X.2009.00558.x.

53. Stamberger H, Nikanorova M, Willemsen MH, et al. STXBP1 encephalopathy: A neurodevelopmental disorder including epilepsy. *Neurology*. 2016;86:954–962. doi: 10.1212/WNL.0000000000002457.

54. Smith NL, Rice KM, Bovill EG, et al. Genetic variation associated with plasma von Willebrand factor levels and the risk of incident venous thrombosis. *Blood*. 2011;117:6007–6011. doi: 10.1182/blood-2010-10-315473.

55. Sharma N, Low SH, Misra S, Pallavi B, Weimbs T. Apical targeting of syntaxin 3 is essential for epithelial cell polarity. *J Cell Biol*. 2006;173:937–948. doi: 10.1083/jcb.200603132.

56. Knowles BC, Weis VG, Yu S, Roland JT, Williams JA, Alvarado GS, Lapierre LA, Shub MD, Gao N, Goldenring JR. Rab11a regulates syntaxin 3 localization and microvillus assembly in enterocytes. *J Cell Sci*. 2015;128:1617–1626. doi: 10.1242/jcs.163303.

57. Vogel GF, Klee KM, Janecke AR, Müller T, Hess MW, Huber LA. Cargo-selective apical exocytosis in epithelial cells is conducted by Myo5B, Slp4a, Vamp7, and Syntaxin 3. *J Cell Biol*. 2015;211:587–604. doi: 10.1083/jcb.201506112.

58. Zupancic G, Ogden D, Magnus CJ, Wheeler-Jones C, Carter TD. Differential exocytosis from human endothelial cells evoked by high intracellular Ca(2+) concentration. *J Physiol*. 2002;544(pt 3):741–755.

59. Valentijn KM, van Driel LF, Mourik MJ, Hendriks GJ, Arends TJ, Koster AJ, Valentijn JA. Multigranular exocytosis of Weibel-Palade bodies in vascular endothelial cells. *Blood*. 2010;116:1807–1816. doi: 10.1182/blood-2010-03-274209.

60. Kiskin NI, Babich V, Knipe L, Hannah MJ, Carter T. Differential cargo mobilisation within Weibel-Palade bodies after transient fusion with the plasma membrane. *PLoS One*. 2014;9:e108093. doi: 10.1371/journal.pone.0108093.

61. Stevenson NL, White IJ, McCormack JJ, Robinson C, Cutler DF, Nightingale TD. Clathrin-mediated post-fusion membrane retrieval influences the exocytic mode of endothelial Weibel-Palade bodies. *J Cell Sci*. 2017;130:2591–2605. doi: 10.1242/jcs.200840.

62. Gaisano HY, Ghai M, Malkus PN, Sheu L, Bouquillon A, Bennett MK, Trimble WS. Distinct cellular locations of the syntaxin family of proteins in rat pancreatic acinar cells. *Mol Biol Cell*. 1996;7:2019–2027.

63. Brochetta C, Suzuki R, Vita F, Soranzo MR, Claver J, Madjene LC, Attout T, Vitte J, Varin-Blank N, Zabucchi G, Rivera J, Blank U. Munc18-2 and syntaxin 3 control distinct essential steps in mast cell degranulation. *J Immunol*. 2014;192:41–51. doi: 10.4049/jimmunol.1301277.

64. Behrendorff N, Dolai S, Hong W, Gaisano HY, Thorn P. Vesicle-associated membrane protein 8 (VAMP8) is a SNARE (soluble N-ethylmaleimide-sensitive factor attachment protein receptor) selectively required for sequential granule-to-granule fusion. *J Biol Chem*. 2011;286:29627–29634. doi: 10.1074/jbc.M111.265199.

65. Zhu D, Koo E, Kwan E, Kang Y, Park S, Xie H, Sugita S, Gaisano HY. Syntaxin-3 regulates newcomer insulin granule exocytosis and compound fusion in pancreatic beta cells. *Diabetologia*. 2013;56:359–369. doi: 10.1007/s00125-012-2757-0.

66. Hafez I, Stolpe A, Lindau M. Compound exocytosis and cumulative fusion in eosinophils. *J Biol Chem*. 2003;278:44921–44928. doi: 10.1074/jbc.M306013200.

Highlights

- Syntaxin-3 is a Weibel-Palade body–associated SNARE (soluble NSF attachment protein receptor) protein that interacts with other Weibel-Palade body–associated SNAREs.
- Blood outgrowth endothelial cells from a variant microvillus inclusion disease patient are an endothelial deficiency model for syntaxin-3.
- Endothelial cells that are deficient for syntaxin-3 have impaired basal and stimulated von Willebrand factor secretion.